Combined Influence of Implant Diameter and Alveolar Ridge Width on Crestal Bone Stress: A Quantitative Approach

Wonjae Yu, DDS, MS, PhD[1]/Yoon-Je Jang, DDS, MS, PhD[2]/Hee-Moon Kyung, DDS, MS, PhD[3]

Purpose: *To quantitatively evaluate the combined influence of implant diameter and alveolar ridge width on crestal bone stress.* ***Materials and Methods:*** *ITI solid-screw implants, 10 mm in length and 3.3, 4.1, and 4.8 mm in diameter, and the alveolar bone were modeled using axisymmetric finite elements. Four different alveolar ridge geometries were selected for each implant: 5-, 6-, 7-, and 8-mm-wide ridges for the 3.3-mm implants; 6-, 7-, 8-, and 9-mm-wide ridges for the 4.1-mm implants; and 7-, 8-, 9-, and 10-mm-wide ridges for the 4.8-mm implants. A nonaxial oblique load of 100 N was applied at 30 degrees to the implant axis. Regression analysis was used to avoid ambiguity when estimating the peak stress occurring at the coronal contact point between the implant and the crestal bone, ie, the singularity point.* ***Results:*** *Peak stresses were dependent on both implant diameter and alveolar ridge width. Substantially lower stresses were recorded around the implants placed in narrower ridges.* ***Conclusion:*** *A regression analysis may be used to quantify the peak stress at the singularity point. An implant with a diameter that is at least half the ridge width is recommended to reduce the stress concentration in the crestal bone.* Int J Oral Maxillofac Implants 2009;24:88–95

Key words: *alveolar ridge width, crestal bone stress, finite element simulation, implant diameter, stress singularity, structural rigidity*

The crestal bone surrounding the implant neck is subject to higher mechanical stresses, which have been observed in many separate studies regardless of differences in implant design,[1–3] loading conditions,[4–7] and/or bone characteristics.[3,8–10] Because stress beyond a certain threshold can result in microdamage and bone resorption according to bone physiology theories,[11] this would seem to suggest that high crestal stress is a plausible cause for crestal bone loss, long-term instability, and even the eventual failure of an implant.[5,6,12–14]

Previous research has focused on the reduction of crestal bone stress through the use of greater diameters or lengths for implants[2,3,15]; novel implant,[14,16,17] abutment,[1,18,19] and thread designs[20,21]; and sophisticated surface modification techniques.[22,23] The common goal in all these approaches has been to increase the bone-to-implant contact area—the load-transmitting area—based on the engineering theory that dividing the load across a larger area can reduce stress. However, the problem is actually more complex, as the high stress in the crestal bone is associated with a stress concentration phenomenon at the sharp corner between the implant and the coronal surface of the crestal bone. The common practice of using the linear elasticity hypothesis for the implant/bone complex may lead to a typical singularity problem. The stress solution at the notch, being inversely proportional to the tip radius, becomes infinite and no unique solution can be determined. This makes both finite element analysis and the interpretation of results problematic.

Although the singularity problem has generally been ignored, some researchers have described the

[1]Assistant Professor, Department of Orthodontics, School of Dentistry, Kyungpook National University, Daegu, Korea.
[2]Private Practice in Daegu, Korea. Clinical Assistant Professor, College of Dentistry, New York University, New York, New York.
[3]Professor, Department of Orthodontics, School of Dentistry, Kyungpook National University, Daegu, Korea.

Correspondence to: Professor Hee-Moon Kyung, Department of Orthodontics, School of Dentistry, Kyungpook National University, 188-1, Samduk 2 Ga, Jung Gu, Daegu 700-412, Korea. Fax: +82-(0)53-421-7607. Email: hmkyung@knu.ac.kr

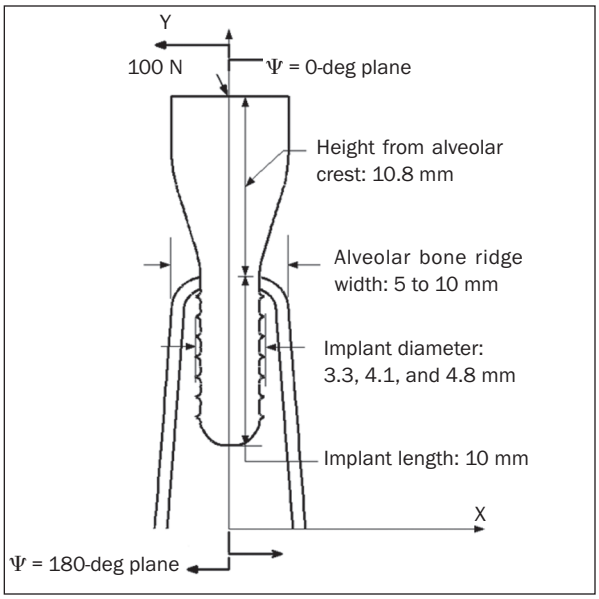

Fig 1 Schematic diagram of ITI solid implant placed in alveolar bone of variable ridge widths.

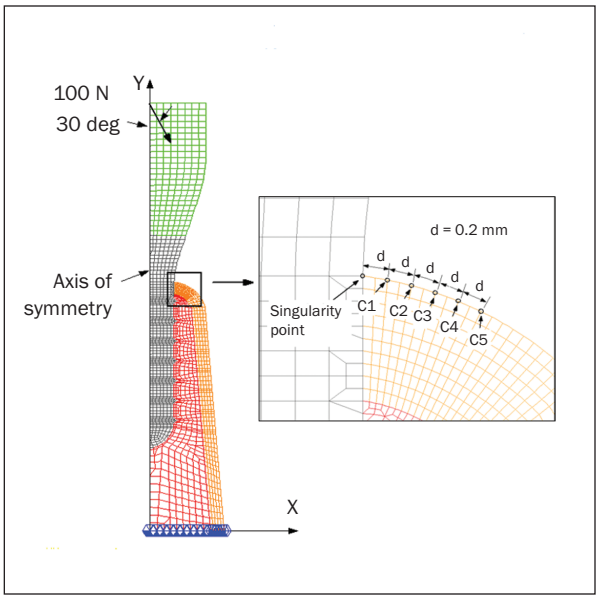

Fig 2 Typical mesh of axisymmetric finite element model (3.3-mm ITI implant placed in 6-mm-wide alveolar ridge).

use of a large number of finite elements.[4,24] However, when a geometric discontinuity is present, mesh refinements only intensify the effect of singularity and diverge the solution, as the exact solution is singular. Even a qualitative comparison may not be entirely free from ambiguity if models with different geometries are studied, since the stresses near the singularity are mesh-dependent.[25,26] This is partly to do with the way finite element mesh models are created: the complicated three-dimensional (3D) geometry of the implant/bone complex dictates the use of an "automesh" procedure, at the expense of proper control of the mesh quality. Thus, to investigate crestal bone stress systematically, a reliable scheme to overcome or circumvent the singularity problem at the sharp corner would appear to be essential.

To reduce the concentration of stress on the crestal bone, the load transmitted from the implant to the crestal bone needs to be controlled, and the key parameter is the structural rigidity of the implant/bone complex at the crestal level, ie, balancing the combined structural rigidity of the implant and crestal bone. Yet, in most previous biomechanical studies, the implant and/or bone has been dealt with in a more individual manner.[5,6,20,24,27] Furthermore, whereas the effects of the internal structure and quality of the alveolar bone have already been investigated,[2,10] the alveolar ridge width, a key ingredient of the bone's structural rigidity, has not been properly addressed.

Accordingly, the purpose of this study is twofold: (*1*) to test a regression analysis method for quantifying the peak stress at the point of singularity in the crestal bone, and (*2*) to investigate the combined and/or interactive influence of implant diameter and alveolar ridge geometry on crestal stress.

MATERALS AND METHODS

Implant and Alveolar Ridge

All the modeled implants had the same length (10 mm), but they varied in diameter (3.3, 4.1, and 4.8 mm; ITI System, Straumann, Waldenburg, Switzerland). The 3.3-mm-diameter implants were placed in alveolar bone with ridge widths of 5, 6, 7, and 8 mm, whereas 6-, 7-, 8-, and 9-mm-wide ridges were selected for the 4.1-mm implants and 7-, 8-, 9-, and 10-mm-wide ridges were modeled for the 4.8-mm implants. Thus, 12 different models were created (Fig 1). The thickness of the cortical shell was fixed at 0.8 mm in all models. The alveolar ridge width was measured at the bone level, corresponding to the first thread of the implant.

Axisymmetric Finite Element Model with Nonaxial Load

To more easily control the mesh characteristics, ie, element size and node locations, an axisymmetric scheme was used to represent the implant/bone complex, and all meshing operations were performed

Table 1 Mechanical Properties of Bone and Implant Materials

Material	Young modulus (GPa)	Poisson ratio
Titanium[39]	102.2	0.35
Cortical bone[10]	13.7	0.3
Cancellous bone[10]	1.37	0.3
Gold (Type IV)[38]	99.3	0.35

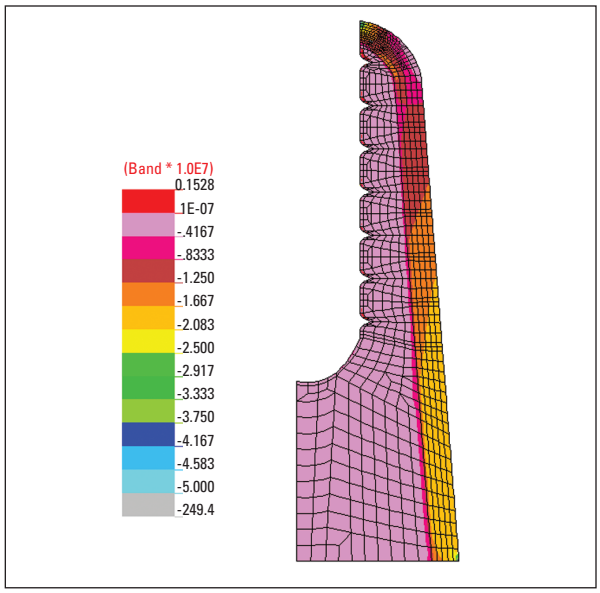

Fig 3 Typical result for overall stress (maximum compressive stresses) distribution (4.1-mm-diameter ITI solid implant placed in 7-mm-wide alveolar ridge).

manually. In the crestal bone, the aspect ratio of each finite element was no greater than 2.0 and the four corner angles for each element were close to 90 degrees. With the exception of a few locations, the element aspect ratio was controlled to within 5.0 throughout the model.

A smooth spline curve was used to model the contour of the alveolar bone to avoid unnecessary increases in stress. Alveolar bone with a height of 15 mm, ie, 1.5 times the implant's endosseous length, was included in the finite element model. To represent osseointegration, the implants were assumed to be rigidly anchored along their entire interface with the bone.

Figure 2 shows an example of the finite element mesh model. The software used was a PC-based NISA II/Display III program (v. 10.0, EMRC, Troy, MI). All the models were created using an 8-node quadrilateral element, ie, NKTP Type 34, which allows the modeling of an axisymmetric structure subject to either axial or nonaxial loads. Each finite element model was constructed using an average of 3,000 elements and 8,000 nodes.

A force of 100 N was applied to a node in the center of the crown's occlusal surface, obliquely at 30 degrees to the vertical axis of the implant (Fig 2). All the nodes on the bottom surface of the bone were constrained to establish boundary conditions during the analyses.

Material Properties

All the materials used in the present study were considered to be isotropic, homogeneous, and linearly elastic, while the mechanical properties were taken from the literature[28,29] (Table 1). For the sake of modeling simplicity, a gold-alloy crown with a 1.5-mm occlusal thickness was used over the titanium abutment, although porcelain-fused-to-metal is usually selected as the implant superstructure in clinics. However, previous studies have confirmed that these materials have the same effect on bone and/or implant stresses.[5,30]

Reference Points

For the systematic comparison of crestal stresses, five nodes were selected as the reference points, located at the most coronal surface of the crestal cortical bone (C1, C2, C3, C4, and C5 in Fig 2) and separated from the implant's external wall by 0.2, 0.4, 0.6, 0.8, and 1.0 mm, respectively. A preliminary study was conducted to ensure that all the reference points were placed in the area unaffected by the notch singularity.

Regression Analysis

A statistical approach was used to quantify the peak stress occurring at the point of singularity, ie, at the sharp corner. The singularity problem was avoided with the use of a regression analysis, whereby the peak stress was calculated asymptotically by extrapolating the results recorded at the five reference points (C1 to C5 in Fig 2). The analysis was performed using SPSS WIN 12.0 software (SPSS Inc, Chicago, IL).

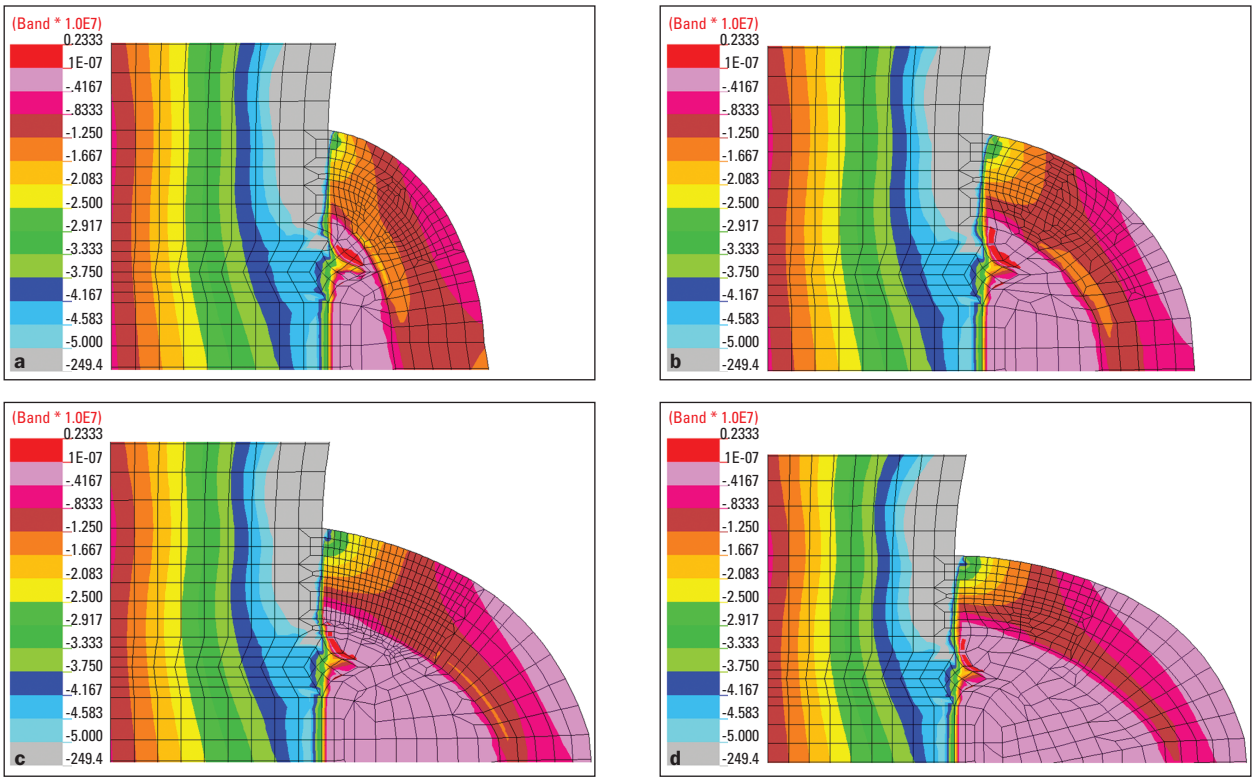

Fig 4 Stress (maximum compressive stresses) distribution in the cervical area (in Pa) around a 4.1-mm ITI implant, placed in alveolar bone of different ridge widths. *a:* 6 mm, *b:* 7 mm, *c:* 8 mm, *d:* 9 mm.

RESULTS

The maximum compressive stress was selected to study the bone loading; the stress distribution was plotted using the built-in visualization tools of the Display III program. In general, the stresses were distributed smoothly throughout the bone, with the exception of the cervical area, which exhibited an acute stress gradient. Figure 3 presents a typical bone stress distribution in the φ = 0-degree plane, obtained from a 4.1-mm-diameter implant placed in a 7-mm-wide ridge. The φ = 0-degree plane was located in the direction of the applied force (Fig 1). Since the compressive stresses in this plane can be produced by both the vertical and lateral components of the obliquely acting force in a superimposed manner, the compressive stress in this plane should be higher than in any other plane around the implant.

Figures 4a to 4d show enlarged views of the crestal region, corresponding to 6-, 7-, 8-, and 9-mm-wide alveolar ridges hosting a 4.1-mm implant. The stresses on the external (most coronal) surface of the crestal bone were highly concentrated in the vicinity of the sharp corner, and the stress concentration varied as a function of the ridge width. The extent and severity of the stress concentration was clearly more significant in the wider ridges.

Instead of the overall profile of the alveolar ridge, the localized geometry close to the crestal area seemed to determine the crestal stresses. As presented in Figs 4a to 4d, the differences in the stress distribution in the bone were minor below the first thread level of the implant for both cortical and cancellous bone. Perceivable differences in stress distribution were observed only in the area near the sharp corner, confirming that the problem of stress concentration was responsible for the high level of stresses in the crestal area.

Similar results were also observed for the 3.3-mm and 4.8-mm implants. Although the stress level varied as a function of either the ridge width or the implant diameter, the crestal bone stress was still lower in the narrower ridges in all three implant models.

The stress values recorded at the five reference points were plotted, as shown in Figs 5a to 5c, along with the estimated peak stresses at the sharp corner, the point of singularity. The stresses at x = 0.0 mm indicate the estimated peak stress based on a regression analysis. The results showed, first, that the stress concentration in the crestal bone area was less significant when implants with the same diameter were hosted in narrower ridges. Second, the crestal stresses were lower when using a wider-diameter implant.

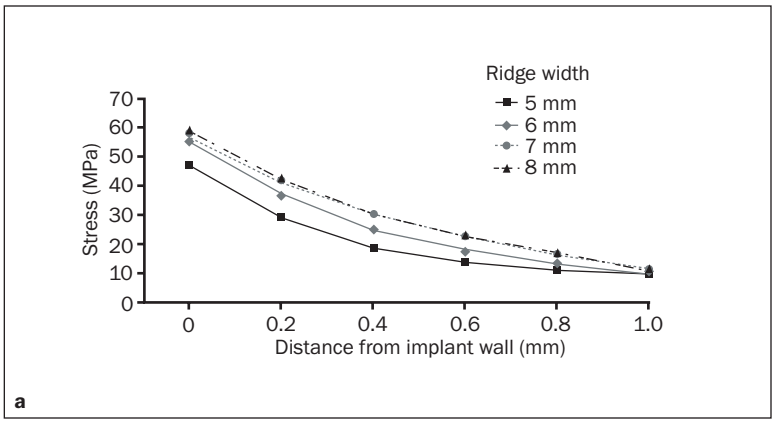

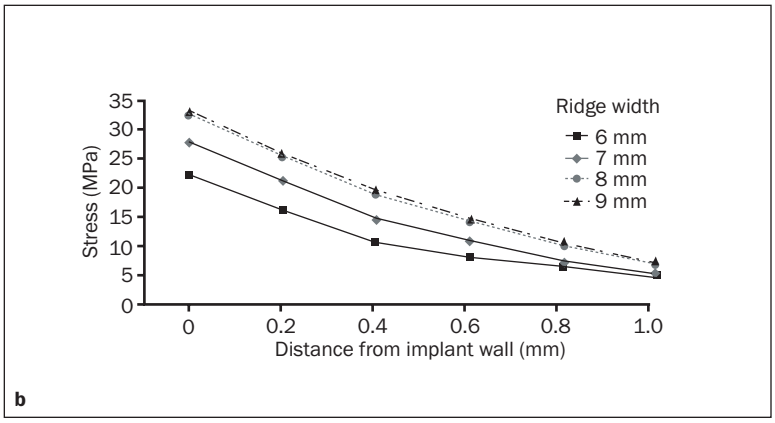

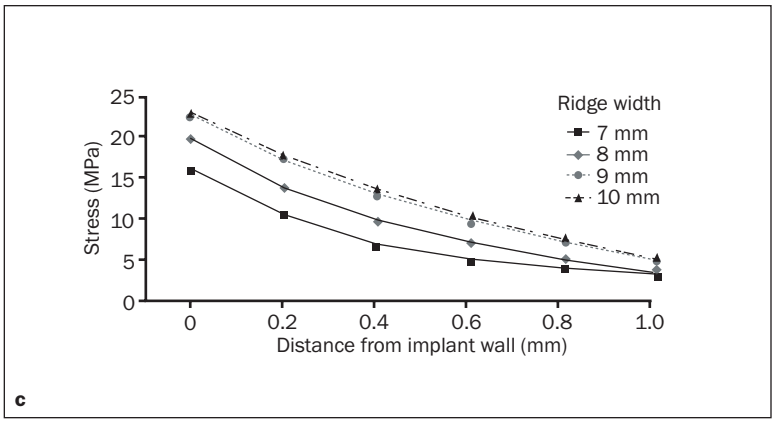

Fig 5 Stresses (maximum compressive stresses) at the coronal surface of cervical cortical bone varying as a function of distance from the bone/implant interface. *a:* 3.3-mm implant, *b:* 4.1-mm implant, *c:* 4.8-mm implant.

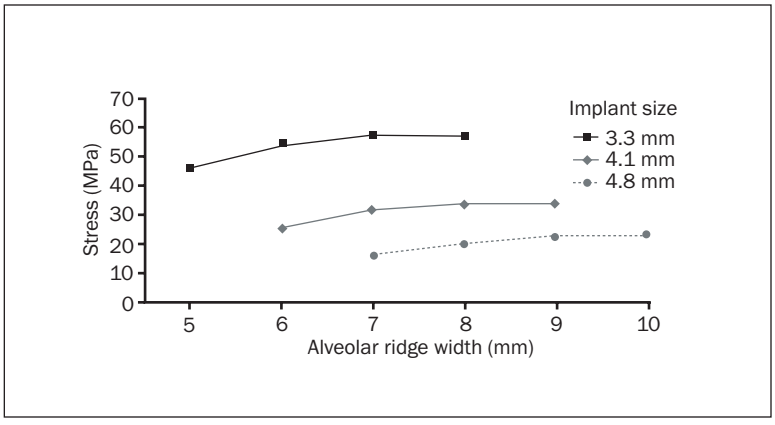

Fig 6 Variation of peak stresses (maximum compressive stresses at singularity point) as a function of implant diameter and ridge width.

Figure 6 shows the estimated peak stress values with respect to the combined effects of implant diameter and ridge width. Essentially, the narrower the ridge width, the lower the peak stress. For the 3.3-mm implant, the peak stress was 46.5 MPa in the narrowest ridge (5 mm), compared to 56.2 MPa in the widest ridge (8 mm). For the 4.1-mm implant, the peak stress was 25.7 MPa in the 6-mm-wide ridge, compared to 34.0 MPa in the 9-mm-wide ridge, and for the 4.8-mm implant, the peak stress was 16.4 MPa in the 7-mm-wide ridge, compared to 22.9 MPa in the 10-mm-wide ridge.

DISCUSSION

When two structural components are connected, continuity in the structural properties is required at the connection to establish a smooth pattern for the load transfer between them. The key parameter is the structural rigidity,[31] which is defined as the product of the elastic modulus (E) and the geometric properties (ie, area, A, and moment of inertia, I) of the constituent components and describes how the material is arranged in space.[32] When structural discontinuity is created so that the structural rigidity changes abruptly at the connection, the load transfer pattern is distorted, resulting in stress concentrations.

The crestal bone may need particular attention, as a discontinuity in the structural rigidity is inevitably created at the juncture of the implant and the crestal bone. The factors determining the variation in the structural rigidity of the implant/bone complex at the crestal bone level need to be carefully addressed because they can play an important role in the crestal stress distribution. Crestal bone stress is already known to be sensitive to such implant factors[2,3,20,21,24] as the diameter, crestal module, and thread design, along with bone factors that include the quality and quantity of the alveolar ridge.[2,5,10] Meanwhile, changes in implant length do not affect the structural rigidity at the crestal bone level, thereby minimizing their influence on crestal stress.[3,20]

The stress concentration in the crestal bone can be attributed to the "notch" effect at the sharp corner between the implant and the crestal bone. In ordinary structures, the stress concentration can be relieved by a smoother design of the notch, for example, increasing the transition radius at the sharp corners. Yet this is clearly not an option for an in vivo structure. One practical way for a clinician to manipulate the structural rigidity of the implant/bone complex is to vary the size (diameter) of the implant relative to the ridge width.

From a stress viewpoint, placement of a wider-diameter implant has a twin effect. First, the increased bone/implant interface area reduces the stress, as per the engineering formula that the stress = load divided by area. Equally important, the difference in the structural rigidity of the implant/bone complex, ie, a more gradual pattern change at the crestal level, effectively reduces the stress concentration. A previous 3D finite element study[3] provides a typical example. When the implant diameter was increased from 3.5 to 6 mm, the crestal bone stress (or strain) was reduced by as much as 3.5-fold instead of 1.7-fold, ie, the number that an elementary theory would yield.

A similar effect can also be achieved when placing implants in narrower alveolar ridges, as a narrower ridge with smaller structural rigidity produces a less abrupt change in the structural rigidity of the implant/bone complex. The results of this study support this idea, as the crestal stresses were obviously lower in the narrower ridges for all three implant models. Because all the other parameters known to affect stress were kept the same, except for the ridge width, the differences in the stress distribution could be correlated with the altered structural rigidity.

Consequently, the balance between implant diameter and alveolar ridge width must be important when controlling the structural rigidity of the implant/bone, implying that these two factors cannot be analyzed independently from each other. However, most previous biomechanical studies have examined the effects of the implant parameters without proper consideration of alveolar ridge width.[3,16,17,24,33] Furthermore, oversimplification of the alveolar crest geometry, for example, using a wide, flat crestal surface that does not reflect the structural rigidity at the crestal bone level in a realistic manner, can exaggerate the stress concentration.

In the present study, the peak stress occurring at the point of singularity was calculated by an extrapolation from the stresses recorded at the reference points (C1 to C5) using a regression analysis (Fig 5). Primary consideration was given to determining the peak stress in a consistent manner. For this, care was taken to avoid placement of reference points within the notch vicinity area, where finite element stress results were affected by the notch singularity. A series of regression analyses was conducted, varying the finite element mesh and the locations of the reference points (C1 to C5), to test the consistency of the regression estimations. The detailed procedures are not included here; however, the results seem promising. The impacts of mesh density and the locations of reference points were minor on the peak stress estimations.

The rapidly varying pattern of the crestal bone stresses near the singularity point required the use of high-order polynomials. Linear, quadratic, and cubic functions were initially tested to simulate the stress distribution pattern. Whereas the lowest stress peak was calculated when using a linear function, the quadratic and cubic functions produced similar results.

Reduction of the peak stress was observed when the alveolar ridge width was less than twice the implant diameter (Fig 6), suggesting that the implant diameter should be at least half the ridge width. Virtually the same pattern was observed for implants under loads with different inclination angles in the range of 0 to 30 degrees. Thus, from a biomechanical standpoint, the wider the implant diameter or the thinner the alveolar ridge, the lower the crestal stress. However, narrower ridges can lead to unfavorable situations. Clinically, thin buccal and/or lingual bone plates are more prone to rapid, horizontal-type bone resorption, which worsens the crown/root ratio, creating a source of increased crestal bone stress, especially when the implant is subject to obliquely acting loads.[6] In contrast, crestal bone resorption can occur in a vertical manner in thicker ridges, creating a cone-shaped bony pocket that effectively reduces the crestal stress concentration.[6,34,35] Therefore, the maximum implant diameter for a given alveolar ridge (or minimum alveolar ridge for an implant) cannot be determined solely on the basis of static biomechanics. Based on clinical experience, the minimum required ridge width is 1.3 to 1.5 times the implant diameter (4.8 mm has been recommended for a 3.3-mm-diameter ITI solid-screw implant and 6.2 mm for a 4.8-mm implant[36]), making a reasonable balance between the implant diameter and the ridge width within a range of 1.3 to 2.0.

Because of the limitations of axisymmetric modeling, the mesiodistal geometry could not be properly addressed. Nonetheless, based on the findings of this study, it can be inferred that the crestal stress in the mesiodistal plane is greater than that in the buccolingual plane, as the distances measured mesiodistally from the implant to adjacent teeth or implants are greater than the buccolingual ridge width. This inference is also supported by a previous 3D analysis[37] in which higher stresses were reported in the mesiodistal plane than in the buccolingual plane. The presence of a bone defect, such as a dehiscence in the buccal or lingual plate, representing a somewhat extreme case of a thin ridge, has been found to lead to increased stress in the mesiodistal plane.[37] However, contradictory results have also been previously reported, in which the stress in the mesiodistal plane was much lower than that in the lingual plane.[38] Thus, since 3D bone stress is a complicated function of various parameters, including the type of load and the nature of the implant/bone interface,[39] further well-designed 3D studies are still needed to address this issue more clearly.

CONCLUSION

This finite element study investigated the effect of different combinations of the implant diameter and alveolar ridge width on crestal bone stresses. The impact of the structural rigidity of the implant/bone complex and its variations was discussed as an important source of crestal bone stress concentration.

Within the limitations of this theoretical study, the following conclusions were drawn:

1. Using the regression analysis method, the peak stress at the sharp corner between the implant and the crestal bone was estimated while avoiding the mesh-dependency problem associated with the notch singularity.
2. The estimated peak stress varied significantly as a function of both implant diameter and alveolar ridge width. This may indicate that the balance of implant diameter and alveolar ridge width needs to be considered in a combined manner. From a biomechanical viewpoint, the wider the implant and the narrower the alveolar ridge, the lower the stress. The reduction in the estimated peak stresses was in the range of 17% to 28%, depending on implant diameter and ridge width.
3. To ensure a decreased level of crestal bone stress, a ratio of implant/alveolar ridge width above 0.5 may be recommended.

REFERENCES

1. Hansson S. The implant neck: Smooth or provided with retention elements. A biomechanical approach. Clin Oral Implants Res 1999;10:394–405.
2. Tada S, Stegaroiu R, Kitamura E, Miyakawa O, Kusakari H. Influence of implant design and bone quality on stress/strain distribution in bone around implants: A 3-dimensional finite element analysis. Int J Oral Maxillofac Implants 2003;18:357–368.
3. Petrie CS, Williams JL. Comparative evaluation of implant designs: Influence of diameter, length, and taper on strains in the alveolar crest. A three-dimensional finite-element analysis. Clin Oral Implants Res 2005;16:486–494.
4. Barbier L, Vander Sloten J, Krzesinski G, Schepers E, Van der Perre G. Finite element analysis of non-axial versus axial loading of oral implants in the mandible of the dog. J Oral Rehabil 1998;25:847–858.

5. Kitamura E, Stegaroiu R, Nomura S, Miyakawa O. Biomechanical aspects of marginal bone resorption around osseointegrated implants: Considerations based on a three-dimensional finite element analysis. Clin Oral Implants Res 2004;15:401–412.
6. Kitamura E, Stegaroiu R, Nomura S, Miyakawa O. Influence of marginal bone resorption on stress around an implant: A three-dimensional finite element analysis. J Oral Rehabil 2005;32:279–286.
7. Natali AN, Pavan PG, Ruggero AL. Analysis of bone-implant interaction phenomena by using a numerical approach. Clin Oral Implants Res 2006;17:67–74.
8. Holmes DC, Loftus JT. Influence of bone quality on stress distribution for endosseous implants. J Oral Implantol 1997;23:104–111.
9. Kitagawa T, Tanimoto Y, Nemoto K, Aida M. Influence of cortical bone quality on stress distribution in bone around dental implant. Dent Mater J 2005;24:219–224.
10. Sevimay M, Turhan F, Kilicarslan MA, Eskitascioglu G. Three-dimensional finite element analysis of the effect of different bone quality on stress distribution in an implant-supported crown. J Prosthet Dent 2005;93:227–234.
11. Frost HM. A 2003 update of bone physiology and Wolff's Law for clinicians. Angle Orthod 2004;74:3–15.
12. Albrektsson T, Zarb G, Worthington P, Eriksson AR. The long-term efficacy of currently used dental implants: A review and proposed criteria for success. Int J Oral Maxillofac Implants 1986;1:11–25.
13. Hoshaw SJ, Brunski JB, Cochran GVB. Mechanical loading of Brånemark implants affects interfacial bone modeling and remodeling. Int J Oral Maxillofac Implants 1994;9:345–360.
14. Meijer HJ, Starmans FJ, Steen WH, Bosman F. Location of implants in the interforaminal region of the mandible and the consequences for the design of the superstructure. J Oral Rehabil 1994;21:47–56.
15. Hanggi MP, Hanggi DC, Schoolfield JD, Meyer J, Cochran DL, Hermann JS. Crestal bone changes around titanium implants. Part I: A retrospective radiographic evaluation in humans comparing two non-submerged implant designs with different machined collar lengths. J Periodontol 2005;76:791–802.
16. Holmgren EP, Seckinger RJ, Kilgren LM, Mante F. Evaluating parameters of osseointegrated dental implants using finite element analysis: A two-dimensional comparative study examining the effects of implant diameter, implant shape, and load direction. J Oral Implantol 1998;24:80–88.
17. Matsushita Y, Kitoh M, Mizuta K, Ikeda H, Suetsugu T. Two-dimensional FEM analysis of hydroxyapatite implants: Diameter effects on stress distribution. J Oral Implantol 1990;16:6–11.
18. Clelland NL, Gilat A. The effect of abutment angulation on stress transfer for an implant. J Prosthodont 1992;1:24–28.
19. Chun HJ, Shin HS, Han CH, Lee SH. Influence of implant abutment type on stress distribution in bone under various loading conditions using finite element analysis. Int J Oral Maxillofac Implants 2006;21:195–202.
20. Chun HJ, Cheong SY, Han JH, et al. Evaluation of design parameters of osseointegrated dental implants using finite element analysis. J Oral Rehabil 2002;29:565–574.
21. Hansson S, Werke M. The implant thread as a retention element in cortical bone: The effect of thread size and thread profile: A finite element study. J Biomech 2003;36:1247–1258.
22. Gotfredsen K, Berglundh T, Lindhe J. Bone reactions adjacent to titanium implants with different surface characteristics subjected to static load. A study in the dog (II). Clin Oral Implants Res 2001;12:196–201.
23. O'Brien GR, Gonshor A, Balfour A. A 6-year prospective study of 620 stress-diversion surface (SDS) dental implants. J Oral Implantol 2004;30:350–357.
24. Bozkaya D, Muftu S, Muftu A. Evaluation of load transfer characteristics of five different implants in compact bone at different load levels by finite elements analysis. J Prosthet Dent 2004;92:523–530.
25. Kalandiia AI. Remarks on the singularity of elastic solutions near corners. J Appl Math Mech 1969;33:127–131.
26. Liu Y, Murakami S, Kanagawa Y. Mesh-dependence and stress singularity in finite element analysis of creep crack growth by continuum damage mechanics approach. Eur J Mech A Solids 1994;13:395–418.
27. Cehreli MC, Akca K, Iplikcioglu H. Force transmission of one- and two-piece Morse-taper oral implants: A nonlinear finite element analysis. Clin Oral Implants Res 2004;15:481–489.
28. Papavasiliou G, Kamposiora P, Bayne SC, Felton DA. 3D-FEA of osseointegration percentages and patterns on implant-bone interfacial stresses. J Dent 1997;25:485–491.
29. Craig RG, Peyton FA. Elastic and mechanical properties of human dentin. J Dent Res 1958;37:710–718.
30. Stegaroiu R, Kusakari H, Nishiyama S, Miyakawa O. Influence of prosthesis material on stress distribution in bone and implants: A three-dimensional finite element analysis. Int J Oral Maxillofac Implants 1998;13:781–790.
31. Morgan MJ, James DF. Force and moment distributions among osseointegrated dental implants. J Biomech 1995;28:1103–1109.
32. Snyder BD, Hauser-Kara DA, Hipp JA, Zurakowski D, Hecht AC, Gebhardt MC. Predicting fracture through benign skeletal lesions with quantitative computed tomography. J Bone Joint Surg Am 2006;88:55–70.
33. Akca K, Cehreli MC. Biomechanical consequences of progressive marginal bone loss around oral implants: A finite element stress analysis. Med Biol Eng Comput 2006;44:527–535.
34. Akagawa Y, Sato Y, Teixeira ER, Shindoi N, Wadamoto M. A mimic osseointegrated implant model for three-dimensional finite element analysis. J Oral Rehabil 2003;30:41–45.
35. Jung ES, Jo KH, Lee CH. A finite element stress analysis of the bone around implant following cervical bone resorption. J Korean Acad Implant Dent 2003;8:38–47.
36. Buser D, von Arx T, ten Bruggenkate C, Weingart D. Basic surgical principles with ITI implants. Clin Oral Implants Res 2000;11(suppl 1):59–68.
37. Van Oosterwyck H, Duyck J, Vander Sloten J, Van Der Perre G, Naert I. Peri-implant bone tissue strains in cases of dehiscence: A finite element study. Clin Oral Implants Res 2002;13:327–333.
38. Clelland NL, Ismail YH, Zaki HS, Pipko D. Three-dimensional finite element stress analysis in and around the Screw-Vent implant. Int J Oral Maxillofac Implants 1991;6:391–398.
39. Geng JP, Tan KB, Liu GR. Application of finite element analysis in implant dentistry: A review of the literature. J Prosthet Dent 2001;85:585–598.